

Environmental DataCube for Open Ocean Aquaculture Evaluation in Southland, New Zealand

Report prepared for the Ministry of Primary Industries

Prepared by:	Guedes, Durrant, McComb and Zyngfogel
Reviewed by:	McComb
Date:	20/07/2021
Revision:	Rev0 – approved for release
Reference No.:	P21-01



TABLE OF CONTENTS

1.	Introduction	1
2.	Methodology.....	2
2.1.	Bathymetry.....	2
2.2.	Winds.....	2
2.3.	Waves.....	6
2.4.	Currents and water properties	8
3.	Spatial statistics	10
3.1.	Bathymetry.....	10
3.2.	Winds.....	11
3.3.	Waves.....	12
3.4.	Currents and water properties	13
4.	Data access	18
5.	References.....	20

LIST OF FIGURES

Figure 2.1	Aerial image of the Stewart Island / Southland region, showing bathymetry derived from the NIWA 250 m gridded dataset.	2
Figure 2.2	Example showing the CCAM model gridding scheme.	3
Figure 2.3	Validation of the downscaled CCAM hindcast against observations from the Invercargill Airport AWS during 2012. Left plots show the times series of measured and modelled u-component wind vector, while the right plot shows the v-component. Dashed is observed, blue is modelled.	4
Figure 2.4	Surface wind speed maps showing the benefit of downscaling with CCAM. Left plots are native winds from ERA5, while the right plots are the same event after dynamical downscaling to 4 km resolution. Shown here are A) the passage of a frontal system, B) lee waves formed by the topographic relief of Stewart Island, C) improved sheltering effect of the island, and D) the influence of the mainland in easterly conditions.	5
Figure 2.5	Southland wave model validation against satellite altimetry data for 2016. Colours indicate density of data points. Regression line is shown in red.	7
Figure 2.6	Output locations for frequency-direction wave spectra.	7
Figure 2.7	Aerial image showing the extent and resolution of the SCHISM hydrodynamical model domain for the Southland region.	8
Figure 2.8	Comparison between water temperature (top) and elevation (bottom) from an oceanographic mooring in Port Adventure, Stewart Island (blue) and SCHISM results (red) from September 2015. Note the tidal amplitudes are well represented by the model, and the trend in surface water temperature is being replicated.	9
Figure 2.9	Comparison between elevation measured by the tide gauge in Bluff Harbour (blue) and the SCHISM results (red). Note that while the model resolution has not been optimised for the harbour dynamics, the tidal regime is reasonably well represented.	9
Figure 3.1	Contours of bathymetry (0-100 m) based on the NIWA 250 m gridded depths.	10
Figure 3.2	Annual mean wind speed at 10 m elevation.	11
Figure 3.3	Decadal P99 wind speed at 10 m elevation.	11
Figure 3.4	Annual mean significant wave height.	12
Figure 3.5	Annual mean peak wave period.	12
Figure 3.6	Decadal maximum significant wave height.	13
Figure 3.7	Depth averaged tidal currents for Spring conditions (M2+S2).	13
Figure 3.8	Annual mean total current speed (tidal and non-tidal) at the sea surface.	14
Figure 3.9	Annual mean total current speed (tidal and non-tidal) at 20 m depth.	14
Figure 3.10	Annual mean total current speed (tidal and non-tidal) at 40 m depth.	15
Figure 3.11	Annual minimum water temperature at the sea surface.	15
Figure 3.12	Annual maximum water temperature at the sea surface.	16
Figure 3.13	Annual minimum water temperature at 20 m depth.	16
Figure 3.14	Annual maximum water temperature at 20 m depth.	17
Figure 3.15	Annual mean salinity at the sea surface.	17
Figure 4.1	User Interface (UI) for the Oceanum data service.	19

1. INTRODUCTION

The Ministry of Primary Industries (MPI) has commissioned an historical recreation of the wind, wave, current and water properties in the Southland region of New Zealand. The purpose of this hindcast is to facilitate the characterisation, with due confidence, of the main physical environmental conditions when considering future regional open ocean aquaculture developments. This includes the range of important ocean properties and metocean conditions that influence aquaculture site selection, and will ultimately govern the design, installation, and safe operation of an offshore facility.

To achieve this objective, a suite of numerical models has been used to hindcast the atmospheric and oceanographic conditions over a contemporary decade, with the information archived within a DataCube for subsequent studies and environmental assessments.

This is an interim report, issued to support the release of the hindcast Datacube. Once potential farm sites have been selected and detailed site surveys have been conducted, the data collected from those surveys will be used to validate the hindcast statistics presented here. The report will also be updated with site specific statistics to characterise the individual farm locations and provide guidance for both the design and the operability criteria.

The report is structured as follows. In Section 2 we describe the hindcast modelling methodology that was used. Example spatial statistics are presented in Section 3, which are a subset of the full package of statistics delivered as GIS layers for display in Google Earth. In Section 4 we detail how the cloud-based DataCube can be queried and the data extracted. The references cited are listed in the final Section 5 of the report. Rose plots for wave, wind and current at a representative location are provided in the Appendix.

2. METHODOLOGY

2.1. Bathymetry

Bathymetric maps of the project area have been created from the NIWA New Zealand bathymetry dataset (Mitchell et al., 2012). This dataset was created using multibeam and single beam sources, as well as historical nautical charts (Figure 2.1). The data are distributed by NIWA under Attribution-NoNavigation-NonCommercial-ShareAlike license (NODL BY-NN-NC-SA 1.0).

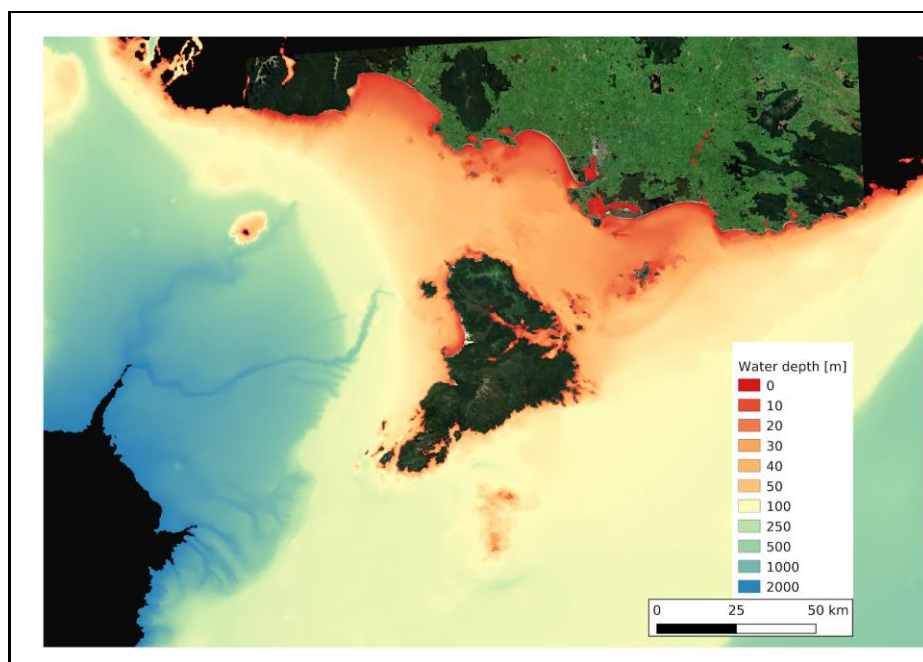


Figure 2.1 Aerial image of the Stewart Island / Southland region, showing bathymetry derived from the NIWA 250 m gridded dataset.

2.2. Winds

The CCAM model has been used to dynamically downscale the ERA5 global reanalysis wind product (ECMWF, 2019) to produce a high-resolution hindcast for the Southland region - including all of Stewart Island. Regional atmospheric models are widely used for dynamical downscaling from global analyses or simulations to finer-resolution regional length scales to consider the influence of local orography, land use, and appropriately parameterised physics. These models also need to account for the influence of atmospheric conditions outside their regional focus. For this reason, various nudging or boundary nesting techniques have been developed to efficiently assimilate the relevant large-scale information from the coarse-resolution analysis or simulation to the regional atmospheric model.

The Conformal-Cubic Atmospheric Model (CCAM) is primarily developed at the Commonwealth Science and Industrial Research Organisation (CSIRO). CCAM is formulated on a quasi-uniform grid, derived by projecting the panels of a cube onto the surface of the Earth. The conformal-cubic grid was devised on these panels by Rancic et al. (1996) and is isotropic except at the eight singular vertices themselves. An example of the C48 grid is shown in Figure 2.2 (left), having 48 x 48 grid points on each panel and a quasi-uniform resolution of 208 km. In contrast to limited-area

models, CCAM can simulate the regional atmosphere using a stretched conformal cubic grid where the grid is focused on the region of interest. This is demonstrated in Figure 2.2 (right), where the same C48 grid has been stretched to focus on central New Zealand. Since the stretched conformal cubic grid has no lateral boundaries, it can implement scale-selective downscaling in CCAM without the need for any special treatment of simulation boundaries. A short description of CCAM is provided by McGregor and Dix (2001).

For the Southland project, horizontal scales of 4 km were defined and the vertical scales were optimised for the definition of the marine boundary layer dynamics. Wind speeds and directions were produced at hourly intervals over a 10-year period (2010-2019).

The ERA5-CCAM downscaling technique has undergone extensive prior validation in central New Zealand. For the Southland domain, we present validation against one year of observations from the AWS at the Invercargill Airport (Fig. 2.3). Note, here we show the modelled wind at 10 m elevation, while the metadata for the observations states a 1 m elevation.

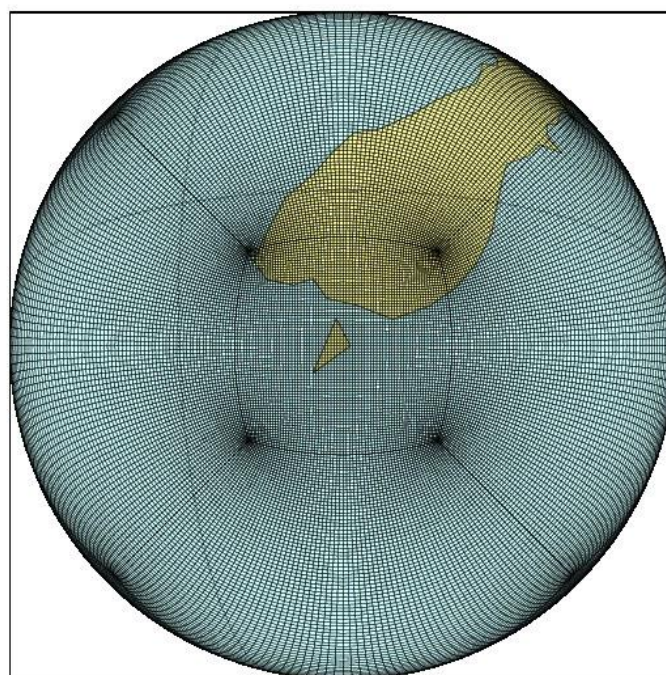


Figure 2.2 Example showing the CCAM model gridding scheme.

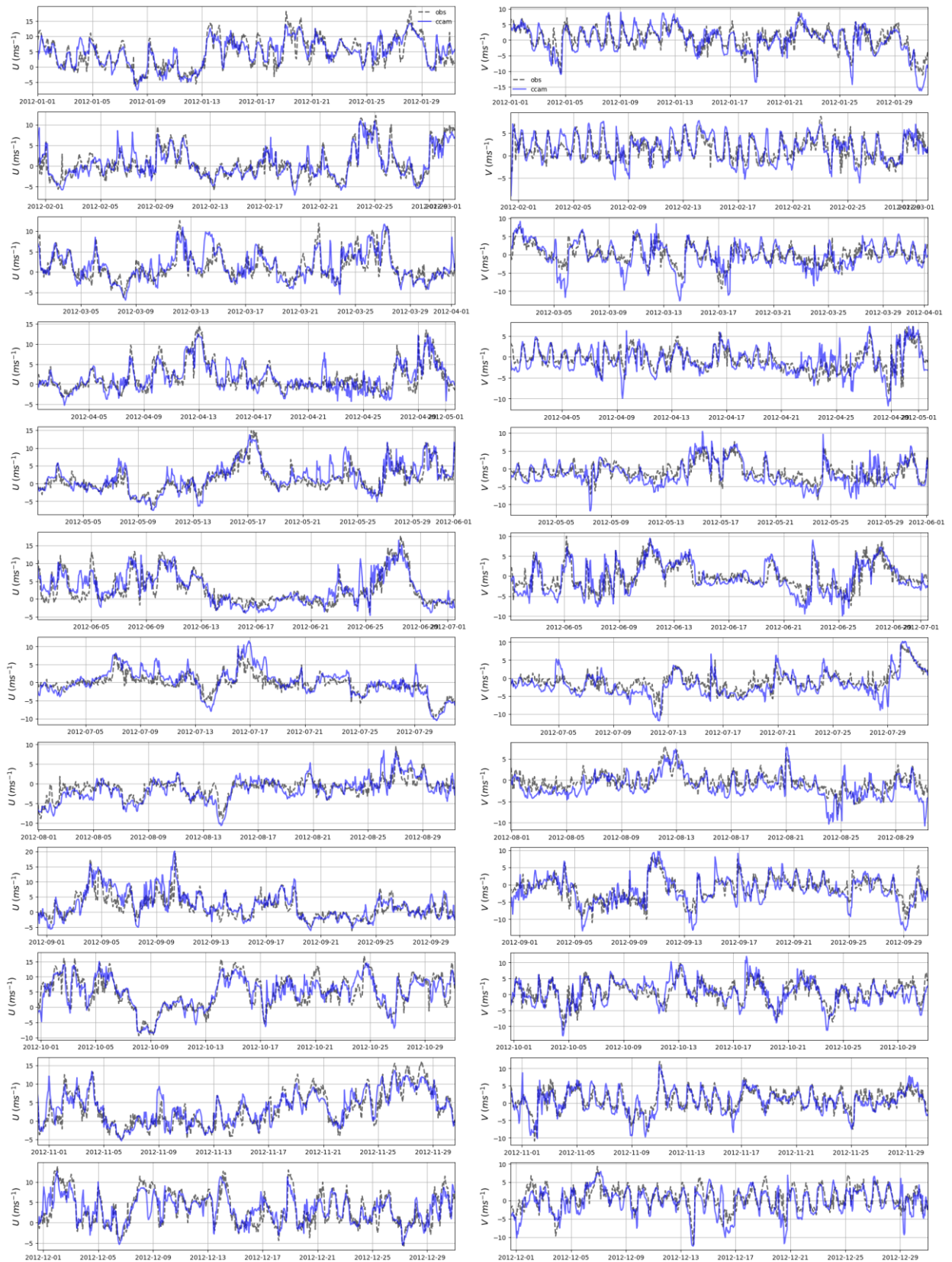


Figure 2.3 Validation of the downscaled CCAM hindcast against observations from the Invercargill Airport AWS during 2012. Left plots show the times series of measured and modelled u-component wind vector, while the right plot shows the v-component. Dashed is observed, blue is modelled.

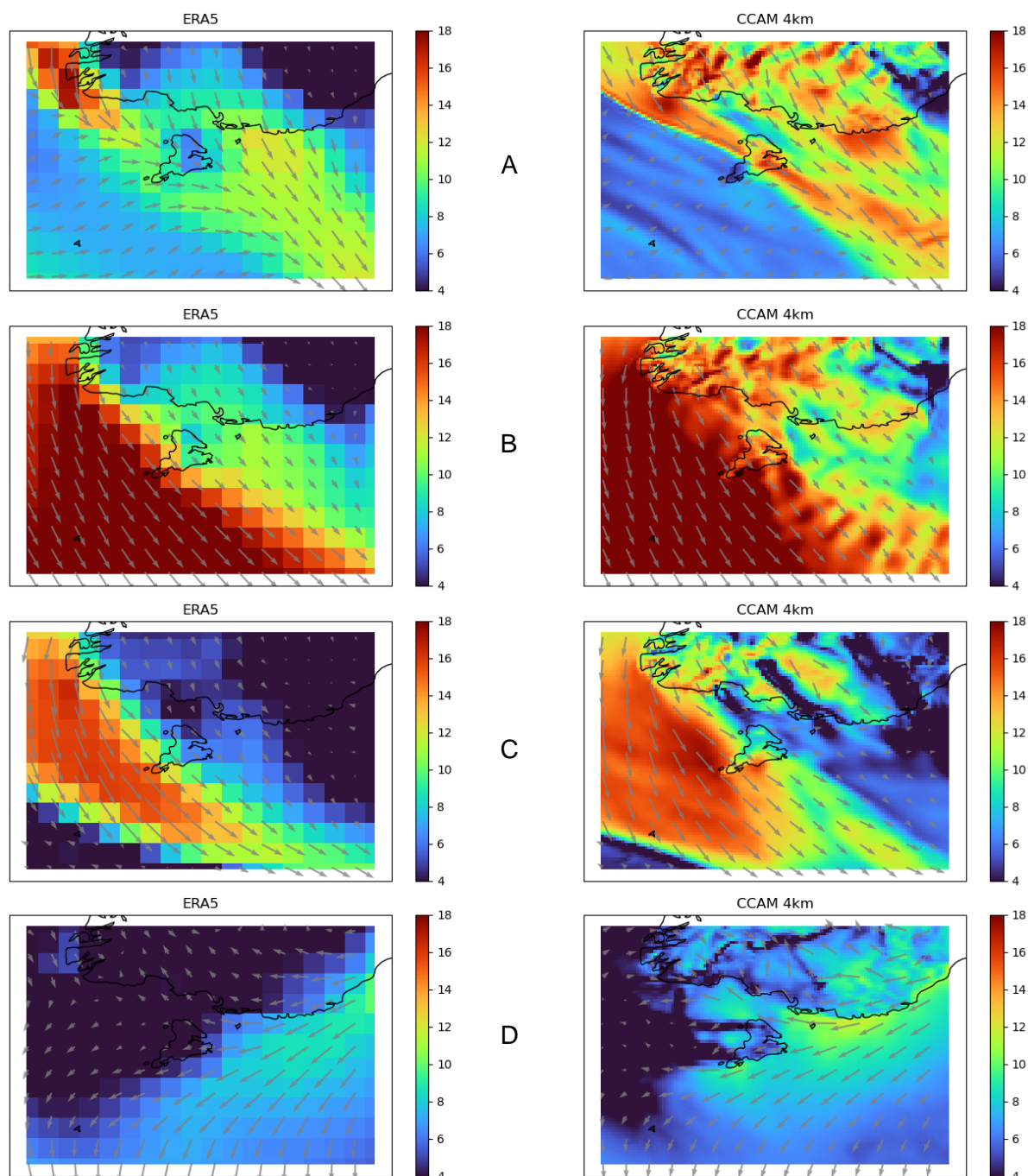


Figure 2.4 Surface wind speed maps showing the benefit of downscaling with CCAM. Left plots are native winds from ERA5, while the right plots are the same event after dynamical downscaling to 4 km resolution. Shown here are A) the passage of a frontal system, B) lee waves formed by the topographic relief of Stewart Island, C) improved sheltering effect of the island, and D) the influence of the mainland in easterly conditions.

2.3. Waves

The wave climate in the project area is complex, often featuring local wind seas from one direction and far-field swells from another and further complicated by the local bathymetry that modulates the wave field through refraction. To accurately quantify the wave climate, a 10-year high-resolution hindcast of the wave conditions was produced for the project, spanning the same period as the CCAM atmospheric hindcast.

The SWAN (Simulating WAVes Nearshore) spectral wave model (Booij et al., 1999) was used for this purpose. SWAN is a third-generation wave action model designed to provide realistic wave parameters from given wind, bottom, tides and current conditions. The model includes formulations for wave growth, refraction, shoaling, nonlinear wave interactions and dissipation by whitecapping, bottom friction and depth-induced wave breaking. SWAN is optimised to model coastal regions, lakes and estuaries but can be used on any scale relevant for wind-generated surface gravity waves. A detailed description of the model equations, parameterisations and numerical schemes can be found in Holthuijsen (2007).

The wave model was run in non-stationary mode using the “ST6” source term parameterisations (Rogers et al., 2012). These source terms have recently been implemented in SWAN and provide improvements to wind input and dissipation under complex conditions of mixed wind sea and swell. Optimal ST6 coefficients were defined in a calibration exercise against regional satellite altimeter data (Fig. 2.5).

For the Southland region, SWAN was run at 1 km resolution, and forced with high-resolution wind fields from the CCAM atmospheric model. Wave boundary conditions were sourced from wave spectra produced from a prior 5 km resolution New Zealand scale hindcast, which was nested inside an existing global hindcast forced by the ERA5 wind reanalysis.

The wave model output included Integrated spectral parameters and frequency-directional wave spectra at hourly intervals. Spectral parameters were archived over the entire model domain at 1 km resolution for 40 different variables representing the combined sea and swell wave field as well as individual sea and swell partitions. Two-dimensional wave spectra were archived over the entire domain at 1241 locations defined using a depth criterion with resolution ranging from 2.5 km in the shallower areas to 10 km in the deeper regions (Fig. 2.6).

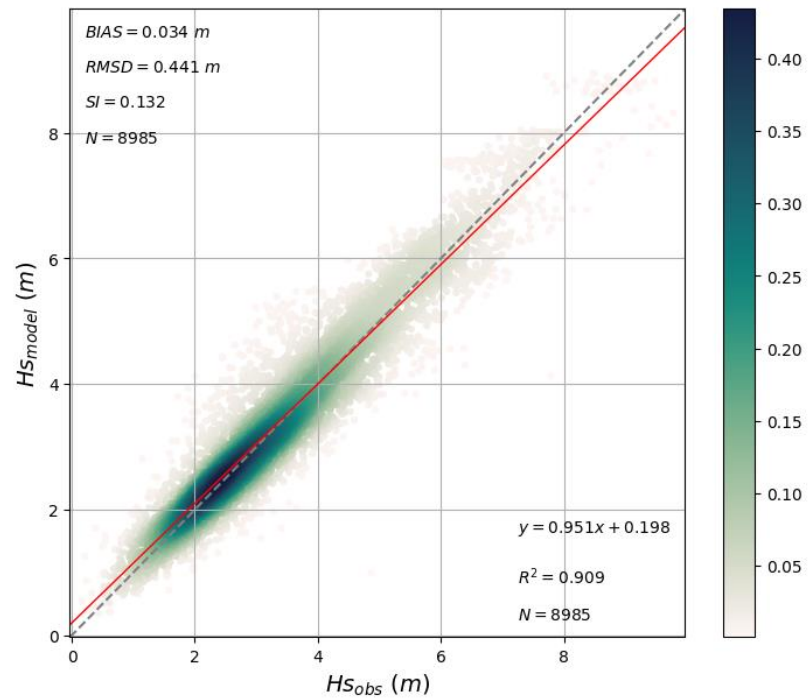


Figure 2.5 Southland wave model validation against satellite altimetry data for 2016. Colours indicate density of data points. Regression line is shown in red.

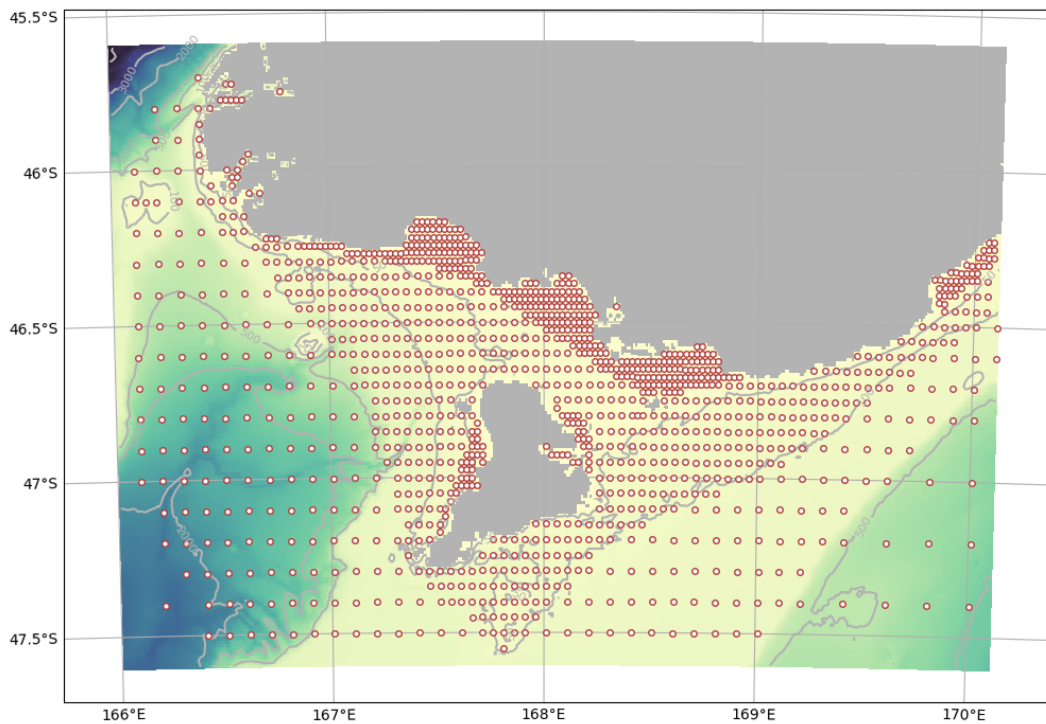


Figure 2.6 Output locations for frequency-direction wave spectra.

2.4. Currents and water properties

The Semi-implicit Cross-scale Hydroscience Integrated System Model (SCHISM) was used to hindcast the oceanic conditions within the project area. An hour-by-hour replication of the three-dimensional flows plus temperature and salinity was completed for the period 2010 to 2019.

SCHISM is a hydrodynamic model (Zhang et al., 2016) based on an unstructured grid (i.e. a triangular mesh), suitable for 2D or 3D baroclinic/barotropic circulation from ocean to coastal regions. A detailed description of the SCHISM model formulation, governing equations and numerics, can be found in the original publication by Zhang and Baptista (2008).

The model grid (Fig. 2.6) has resolution ranging from 1,700 m near the open ocean boundary to 80 m near the coast. For the purpose of this study, the regions east and northeast of Stewart Island were given a higher resolution. SCHISM was run in full 3D baroclinic mode, with 20 vertical sigma layers and 5 z layers below 500 m. Elevation and current amplitudes and phases of the dominant tidal constituents (M2, S2, N2, K2, K1, O1, P1, Q1) were sourced from the OTIS (Oregon State University Tidal Inversion Software) assimilated barotropic model. Residual velocities and water column properties were defined from the global 1/12-degree reanalysis products released by the EU-funded Copernicus Project. Atmospheric forcing (10 m wind speed, temperature, humidity, mean sea-level pressure, precipitation and solar radiation) was sourced from the CCAM downscaling of the ERA5 reanalysis.

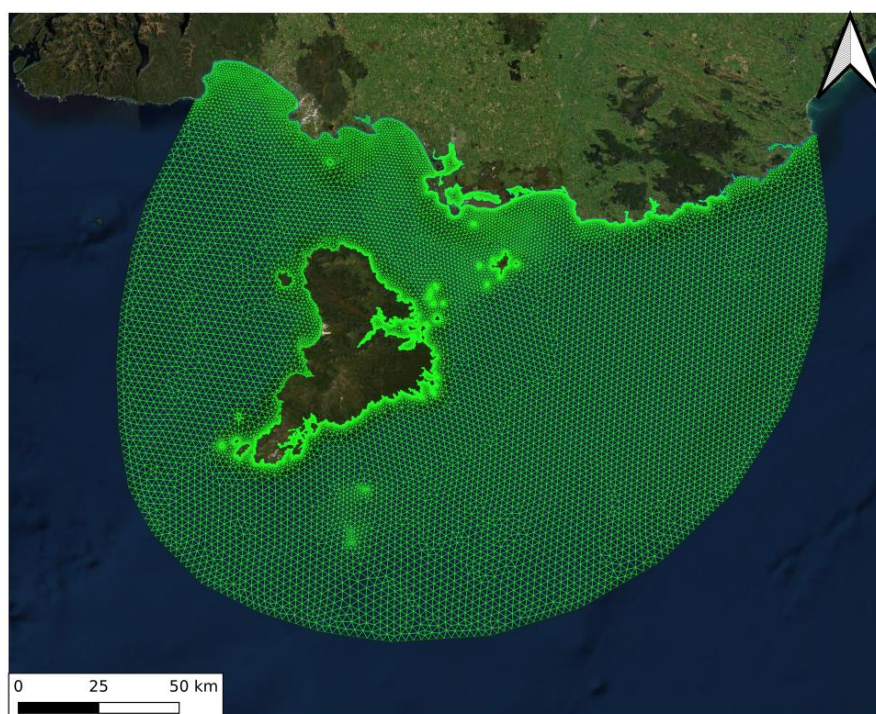


Figure 2.7 Aerial image showing the extent and resolution of the SCHISM hydrodynamical model domain for the Southland region.

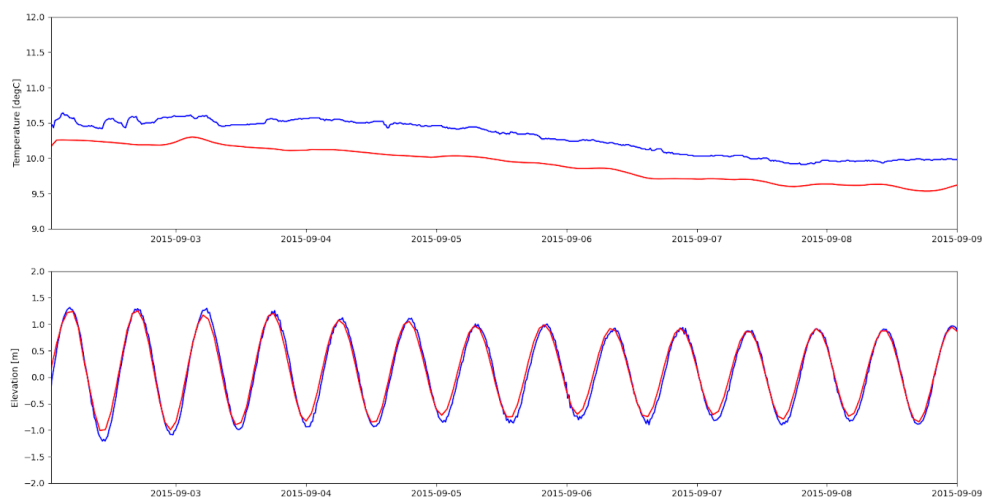


Figure 2.8 Comparison between water temperature (top) and elevation (bottom) from an oceanographic mooring in Port Adventure, Stewart Island (blue) and SCHISM results (red) from September 2015. Note the tidal amplitudes are well represented by the model, and the trend in surface water temperature is being replicated.

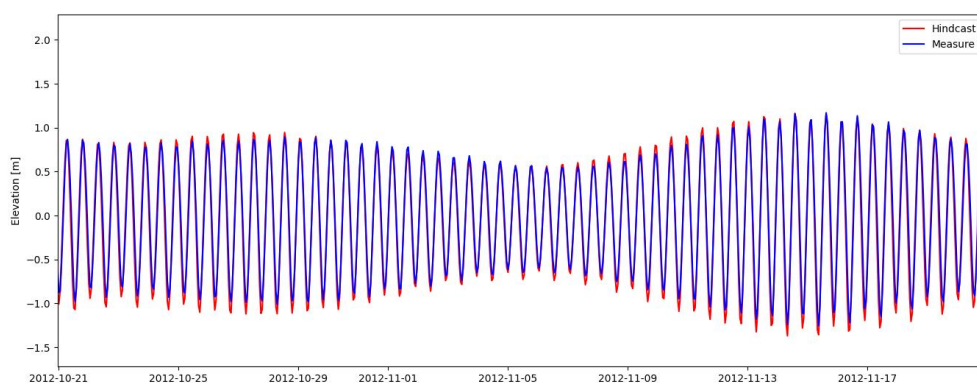


Figure 2.9 Comparison between elevation measured by the tide gauge in Bluff Harbour (blue) and the SCHISM results (red). Note that while the model resolution has not been optimised for the harbour dynamics, the tidal regime is reasonably well represented.

3. SPATIAL STATISTICS

An extensive set of spatial statistics have been prepared from the DataCube, and these are listed as follows:

- Bathymetry in 5 m isobaths.
- Statistics of wind speed - annual and seasonal wind speeds (mean, P50, P90, P99, maximum).
- Statistics of significant wave height - annual and seasonal values (mean, P50, P90, P99, maximum).
- Statistics of the tidal flow regime (maximum depth-averaged).
- Statistics of the combined tidal and non-tidal flow regime - annual values (mean, P50, P90, P99, maximum) for surface layer and 20 m depth.
- Mean annual and seasonal flow streamlines for the total currents (tidal and non-tidal) for the upper 60 m of the water column.
- Statistics (mean, minimum, maximum, standard deviation) of the annual and seasonal temperature and salinity regime at surface and 20 m depth.

These statistics have been produced as layers for display in Google Earth. In the following sections, a selection of those maps is presented as examples.

3.1. Bathymetry

The NIWA 250 m gridded data have been contoured to show the depth increments at 5 m spacing, from 0 to the 100 m isobath. An example is provided in Figure 3.1.

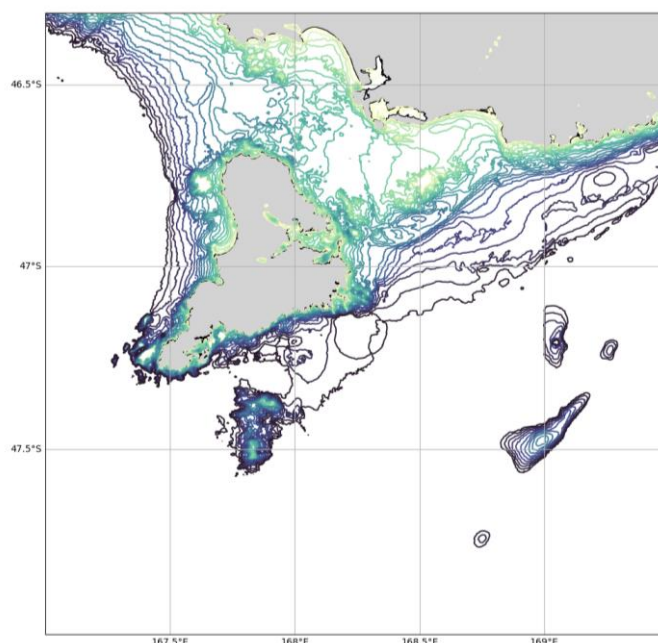


Figure 3.1 Contours of bathymetry (0-100 m) based on the NIWA 250 m gridded depths.

3.2. Winds

Example statistics of the downscaled wind field is presented in Figures 3.2 and 3.3 for the annual mean and decadal P99 speed, respectively.

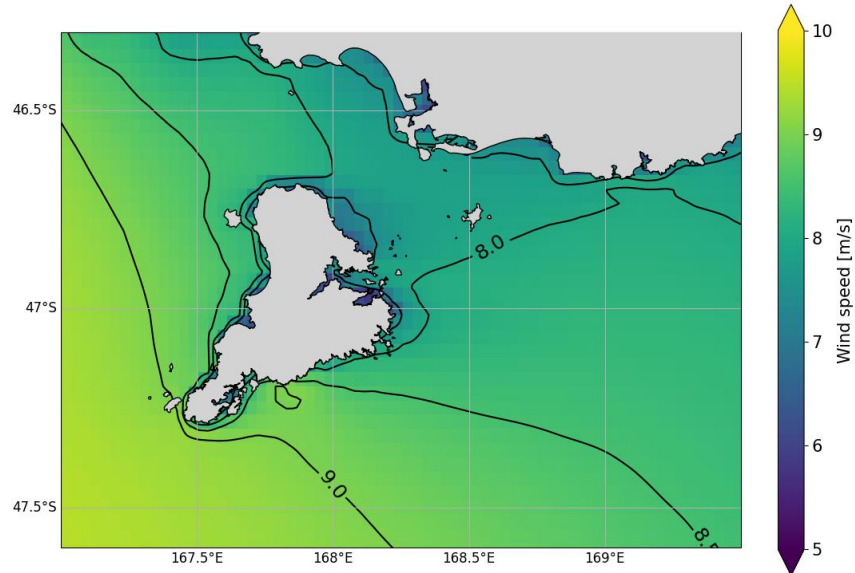


Figure 3.2 Annual mean wind speed at 10 m elevation.

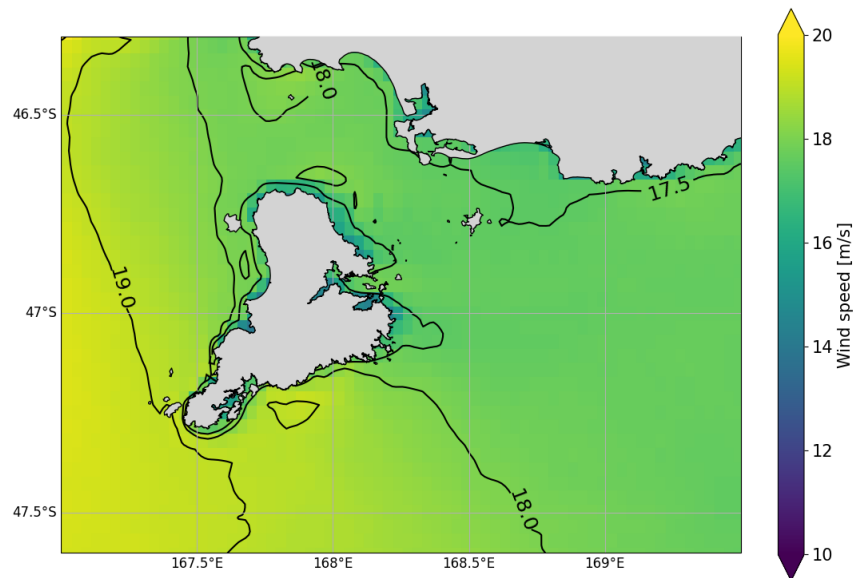


Figure 3.3 Decadal P99 wind speed at 10 m elevation.

3.3. Waves

Example statistics of the regional wave climate are presented in Figures 3.4 - 3.6.

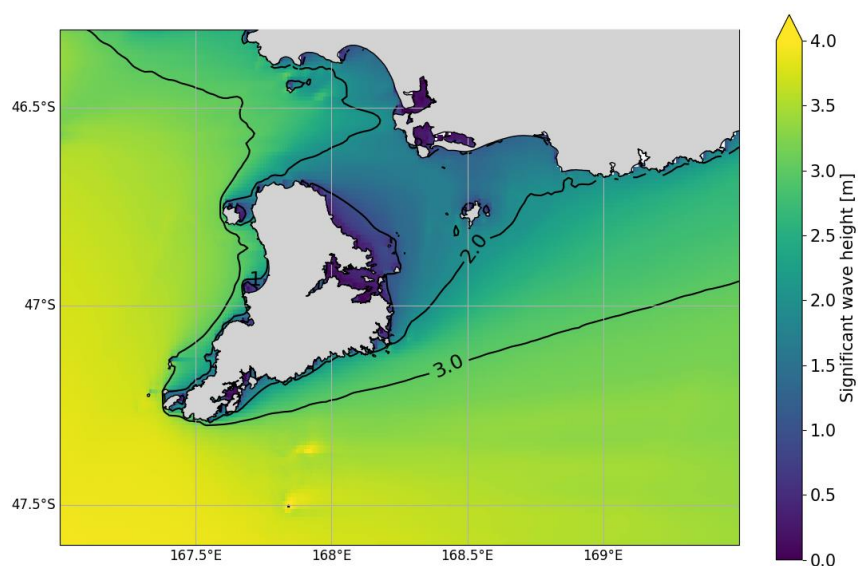


Figure 3.4 Annual mean significant wave height.

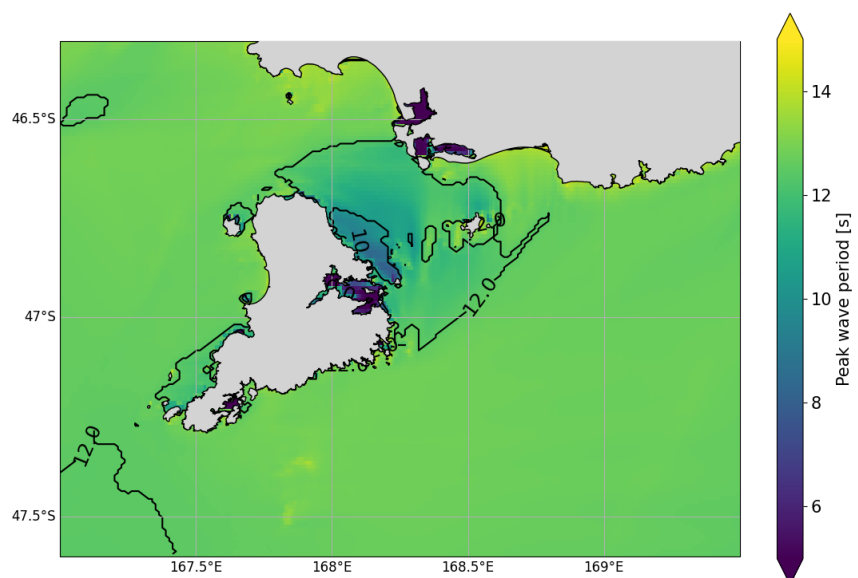


Figure 3.5 Annual mean peak wave period.

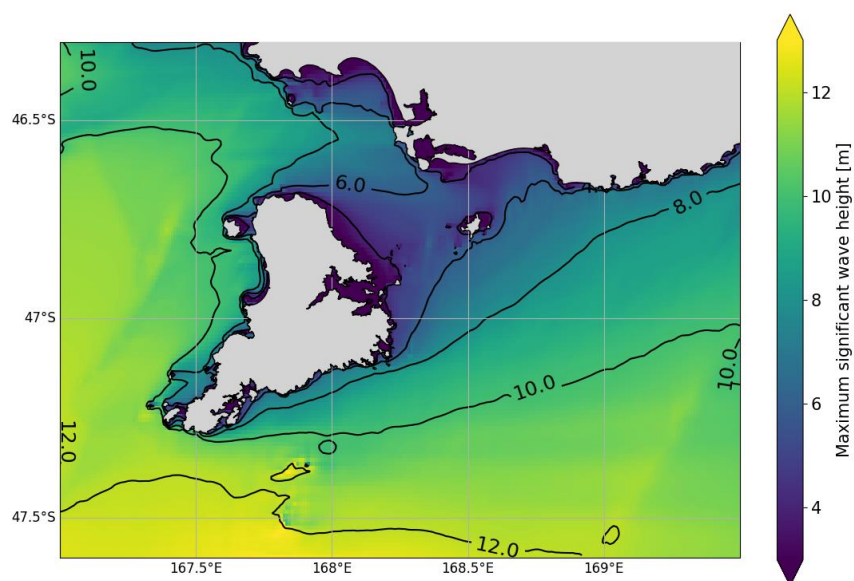


Figure 3.6 Decadal maximum significant wave height.

3.4. Currents and water properties

Example statistics of the regional flow regime are presented in Figures 3.7 - 3.15.

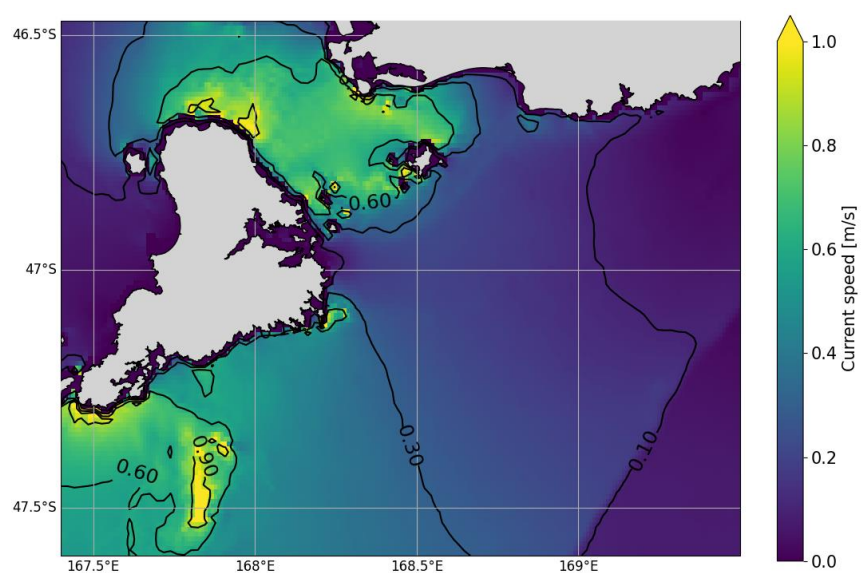


Figure 3.7 Depth averaged tidal currents for Spring conditions (M2+S2).

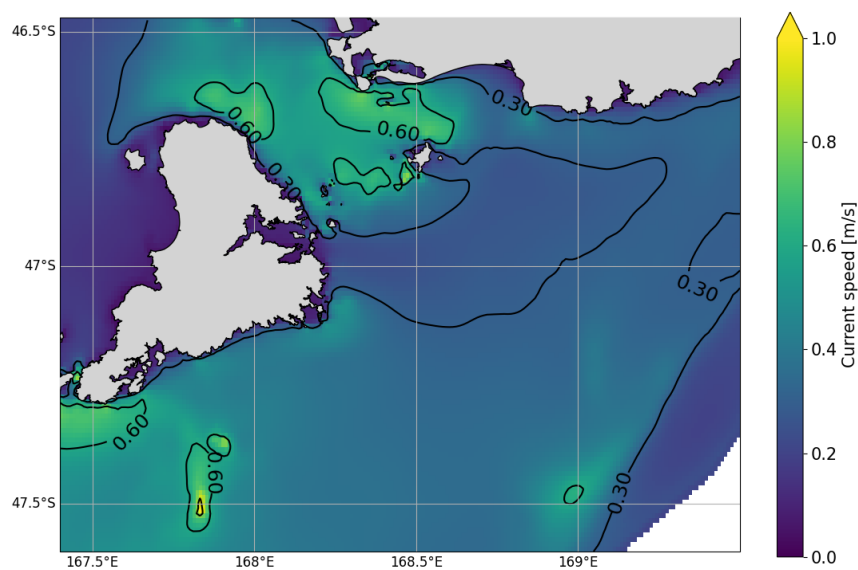


Figure 3.8 Annual mean total current speed (tidal and non-tidal) at the sea surface.

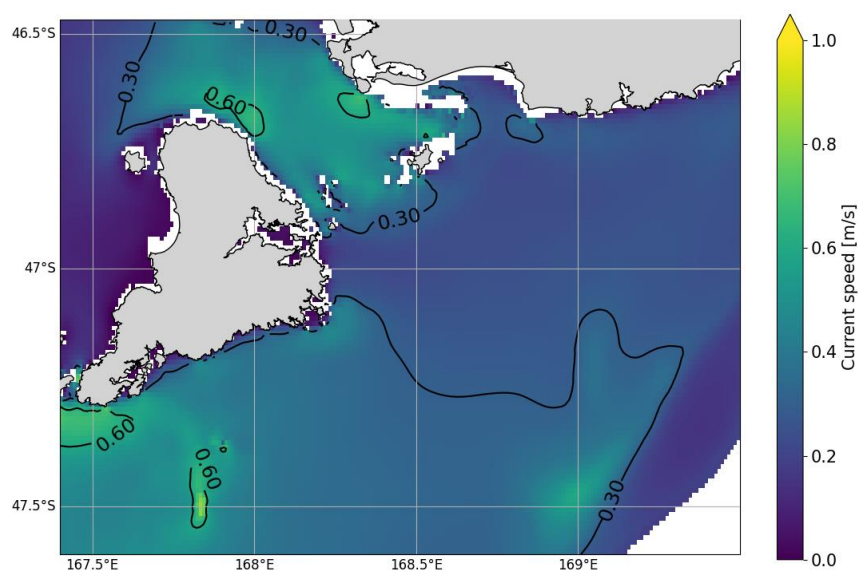


Figure 3.9 Annual mean total current speed (tidal and non-tidal) at 20 m depth.

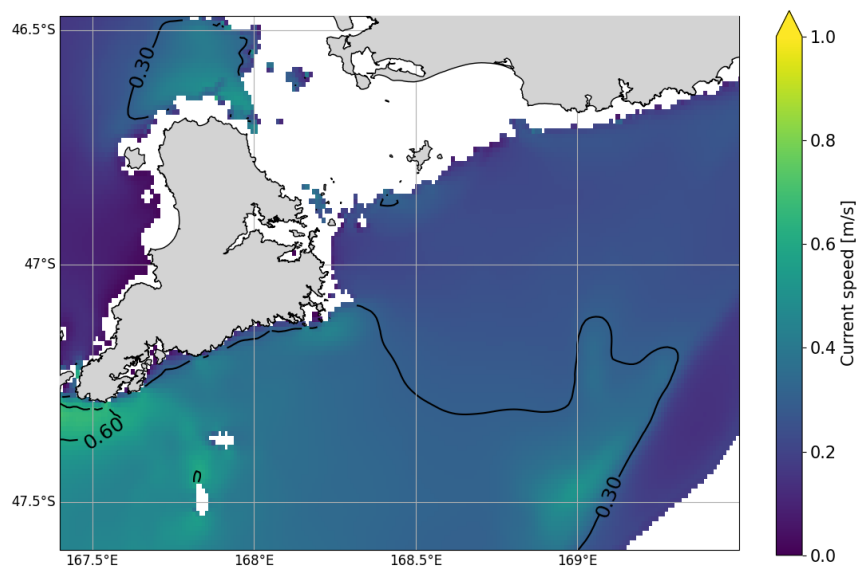


Figure 3.10 Annual mean total current speed (tidal and non-tidal) at 40 m depth.

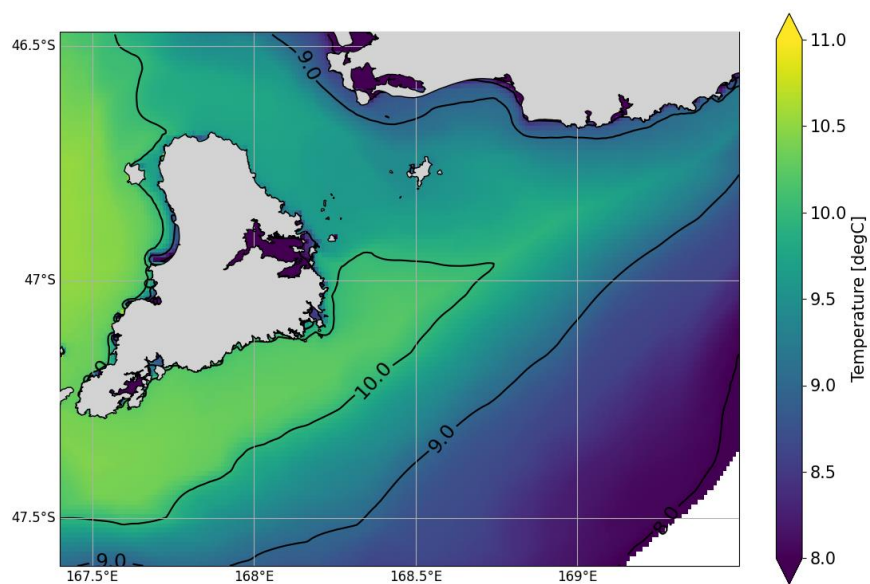


Figure 3.11 Annual minimum water temperature at the sea surface.

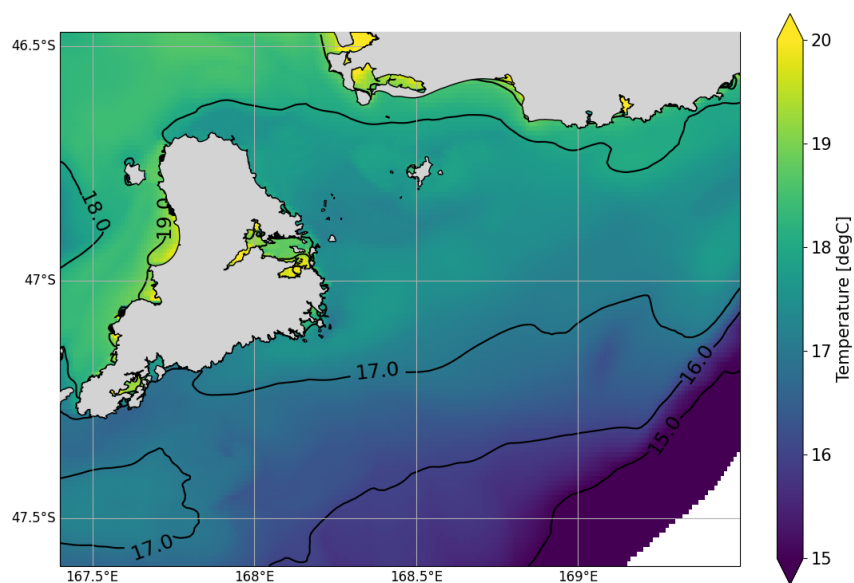


Figure 3.12 Annual maximum water temperature at the sea surface.

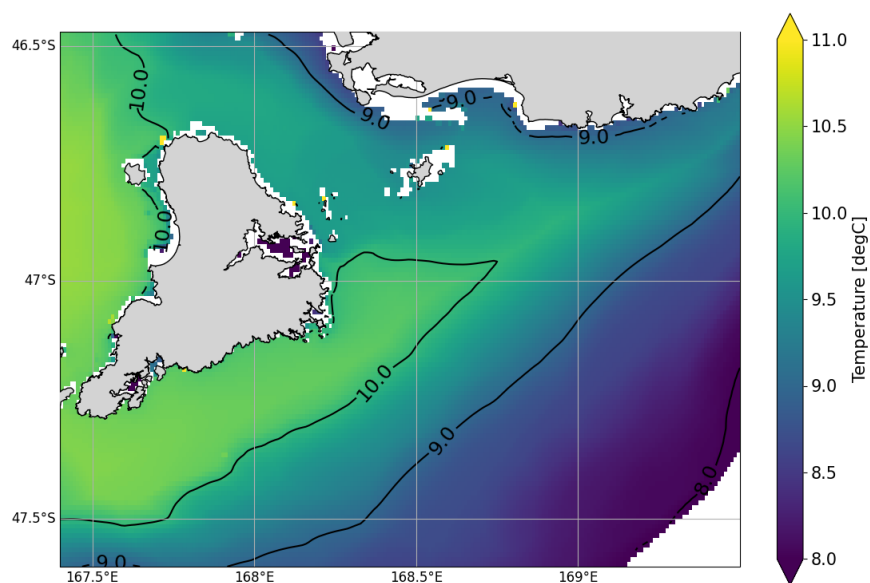


Figure 3.13 Annual minimum water temperature at 20 m depth.

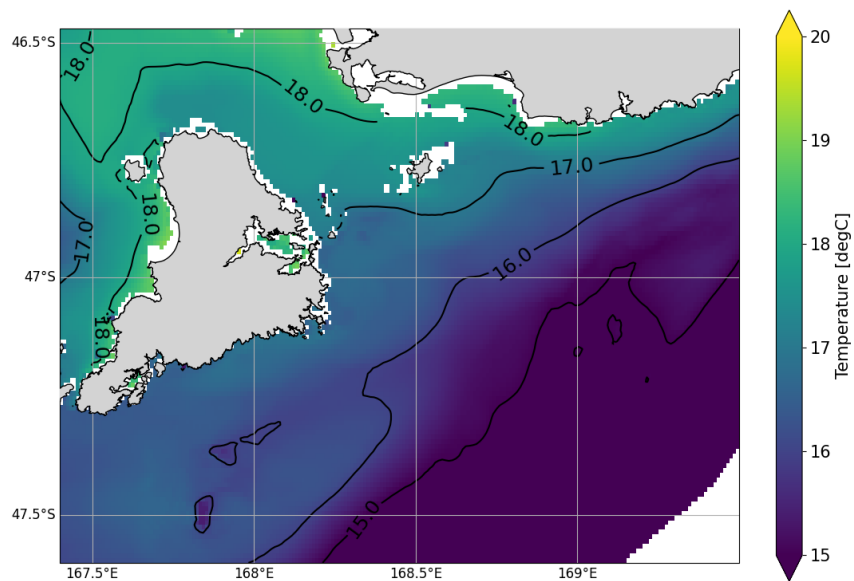


Figure 3.14 Annual maximum water temperature at 20 m depth.

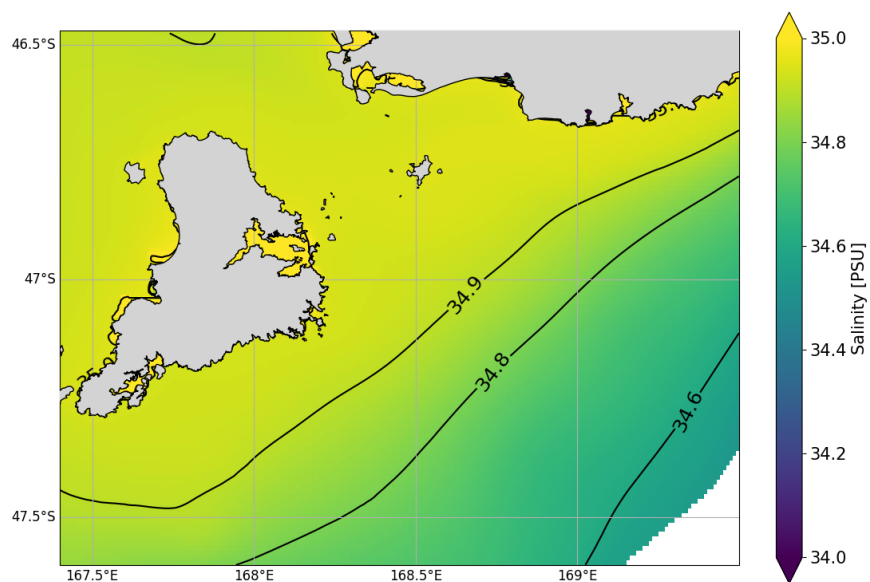


Figure 3.15 Annual mean salinity at the sea surface.

4. DATA ACCESS

The DataCube can be accessed remotely via the Oceanum Data Service, with a request functionality to rapidly download timeseries for any location within the domain. Instructions for the current version of the User Interface (UI) are as follows:

- Go to <https://data.oceanum.io> using a modern browser
- When asked to sign in, create a new account or log in to an existing account
- Use the data access interface to construct a data request:
- Select a dataset - the geographical extent will appear on the map
- Select request type (points or a route)
- Select variables (optional)
- Select time range (optional)
- Select file format
- Choose locations or draw a route on the map
- Press request button to start request

Once the request is complete a download link will appear

An example of the UI is shown in Figure 4.1. Note that the locations can also be edited on the left side of the interface or imported from a CSV delimited file. Future upgrades of the UI may change the details of the workflow but will be supported by documentation and contextual help.

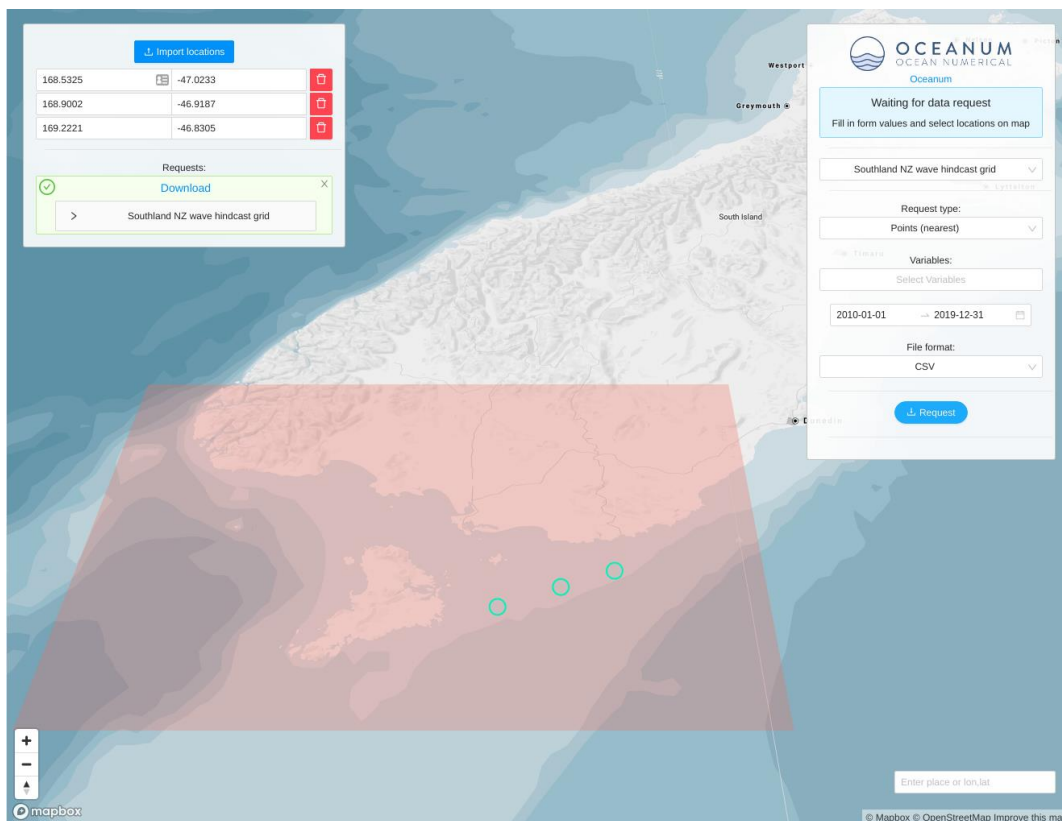
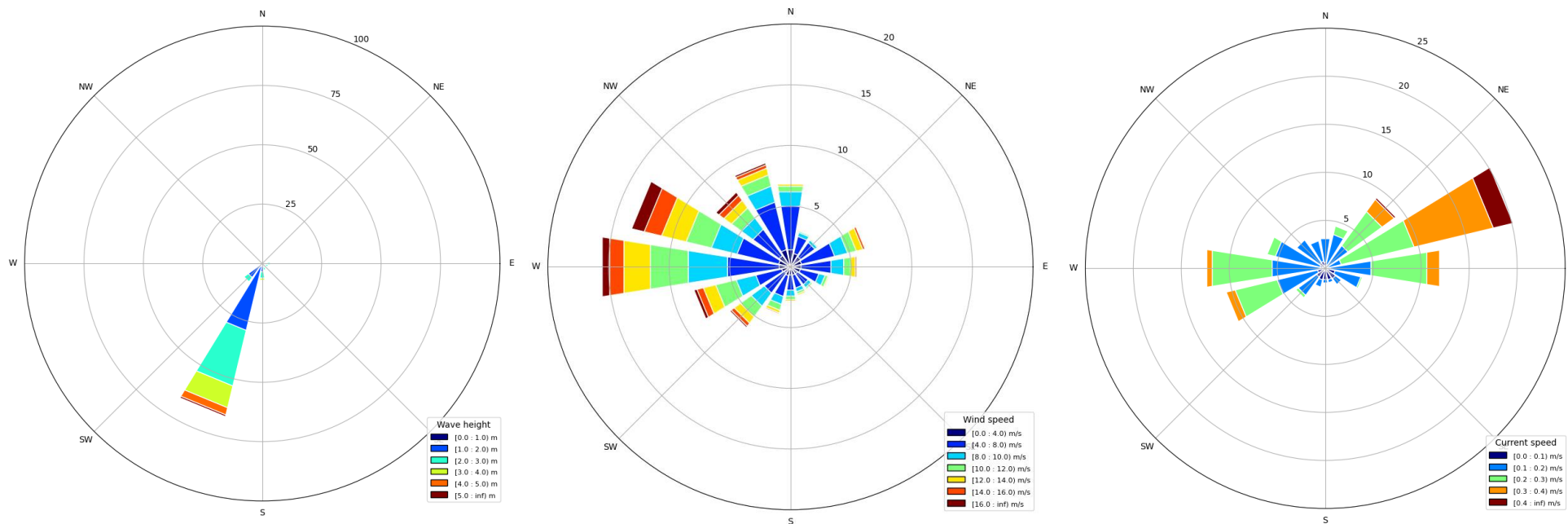


Figure 4.1 User Interface (UI) for the Oceanum data service.

5. REFERENCES

- Booij, N., R. C. Ris, and L. H. Holthuijsen. 1999. "A Third-Generation Wave Model for Coastal Regions: 1. Model Description and Validation." *Journal of Geophysical Research: Oceans* 104 (C4): 7649–66. <https://doi.org/10.1029/98JC02622>.
- ECMWF. 2019. "ERA5: Fifth Generation of ECMWF Atmospheric Reanalyses of the Global Climate." <https://cds.climate.copernicus.eu/cdsapp#!/home>.
- Egbert, Gary D., and Svetlana Y. Erofeeva. 2002. "Efficient Inverse Modeling of Barotropic Ocean Tides." *Journal of Atmospheric and Oceanic Technology* 19 (2): 183–204. [https://doi.org/10.1175/1520-0426\(2002\)019<0183:EIMOBO>2.0.CO;2](https://doi.org/10.1175/1520-0426(2002)019<0183:EIMOBO>2.0.CO;2).
- Holthuijsen, L. H. 2007. *Waves in Oceanic and Coastal Waters*. Cambridge University Press.
- McGregor, J. L., and M. R. Dix, 2008: "An Updated Description of the Conformal-Cubic Atmospheric Model". *High Resolution Numerical Modelling of the Atmosphere and Ocean*, K. Hamilton and W. Ohfuchi, Eds., Springer, 51–75.
- Mitchell, J.S., Mackay, K.A., Neil, H.L., Mackay, E.J., Pallentin, A., Notman P., 2012. *Undersea New Zealand*, 1:5,000,000.
- Rančić, M., R. J. Purser, D. Jović, R. Vasic, and T. Black, 2017. "A Nonhydrostatic Multiscale Model on the Uniform Jacobian Cubed Sphere". *Monthly Weather Review*, 145, 1083–1105, <https://doi.org/10.1175/MWR-D-16-0178.1>.
- Rogers, Erick, Alexander Babanin, and David Wang. 2012. "Observation-Consistent Input and Whitecapping Dissipation in a Model for Wind-Generated Surface Waves: Description and Simple Calculations." *Journal of Atmospheric and Oceanic Technology* 29 (March): 120326124007003. <https://doi.org/10.1175/JTECH-D-11-00092.1>.
- Zhang, Yinglong & Ye, Fei & Stanev, Emil & Grashorn, Sebastian. 2016. "Seamless cross-scale modelling with SCHISM". *Ocean Modelling*. 102. 10.1016/j.ocemod.2016.05.002.
- Zhang, Y. L., and A. M. Baptista. 2008. "A Semi-Implicit Eulerian-Lagrangian Finite Element Model for Cross-Scale Ocean Circulation." *Ocean Modelling* 21: 71–96.

APPENDIX



Rose plots showing the annual wave, wind and surface current directional regime for a location east of Ruapuke Island [46.9, 168.6].